104 (2025) 104600

Contents lists available at ScienceDirect

Poultry Science

journal homepage: www.elsevier.com/locate/psj

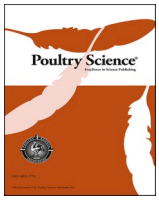

Goose astrovirus induces apoptosis and endoplasmic reticulum stress in gosling hepatocytes

Zhihua Lu [a,1], Haiqin Li [a,b,1], Xiaona Gao [a], Duanfeng Fu [a], Haoyu Huang [a], Cheng Huang [a], Meiqin Wu [a], Xiaoquan Guo [a,*]

[a] Jiangxi Provincial Key Laboratory for Animal Health, College of Animal Science and Technology, Jiangxi Agricultural University, Nanchang, China
[b] Institute of Animal Husbandry and Veterinary Medicine, Jiangxi Academy of Agricultural Sciences, Nanchang, Jiangxi 330200, China

ARTICLE INFO

Keywords:
Goose astrovirus virus
Endoplasmic reticulum stress
Apoptosis
Gosling

ABSTRACT

The ongoing Goose astrovirus (**GoAstV**) epidemic, which primarily infects goslings causing severe liver damage, has inflicted considerable damage on the poultry industry. Endoplasmic reticulum stress (**ERS**) is a significant modulator of several viral infections, while severe ERS may result in apoptosis. This study examined the roles and possible mechanisms of ERS and apoptosis in GoAstV-induced liver injury in goslings. Two hundred Xingguo gray geese were chosen and randomly separated into two groups (Con and Dis). The Dis group received a subcutaneous injection of GoAstV genotype 2 (**GoAstV-2**) JX01 (2×10^6 $TCID_{50}$/0.2 mL), whereas the Con group received a subcutaneous injection of 0.2 mL physiological saline, both at 1 day of life. Subsequent analyses demonstrate that the levels of aspartate aminotransferase (**AST**) and alanine aminotransferase (**ALT**) increased following GoAstV infection. Hematoxylin and eosin (HE) staining revealed swollen and ruptured hepatocytes, with significant inflammatory cell infiltration. Electron microscopy revealed expansion of the endoplasmic reticulum (**ER**) and aggregation of chromatin at the periphery. TUNEL testing further demonstrated an increase in the quantity of positive cells. RT-qPCR and Western blot analyses indicated that GoAstV infection enhanced the expression of ER Ca^{2+} release channels (IP3R and RYR) and calmodulin-dependent protein kinase II (**CaMKII**), while decreasing the expression of ER Ca^{2+} uptake channels (SERCA). Further, GoAstV infection activated ERS-related factors, including GRP78, IRE1α, PERK, ATF6, eIF2α, ATF4, CHOP, TRAF2, and JNK, induced the expression of pro-apoptotic factors (Caspase-3, Caspase-9, and Bax), and inhibited the mRNA and protein expression of the anti-apoptotic factor Bcl-2. Correlation analysis further revealed a potential relationship among ERS gene expression, apoptotic gene expression, and liver injury. In summary, GoAstV infection can lead to liver injury by interfering with ER Ca^{2+} homeostasis, exacerbating ERS and inducing hepatocyte apoptosis.

Introduction

Goose astrovirus (GoAstV), a non-enveloped, single-stranded, positive-sense RNA virus, is a novel avian astrovirus (Xu et al., 2023). This virus was first reported in China in 2016, after which it rapidly spread to other inland provinces (Zhang et al., 2017; Niu et al., 2018; Yang et al., 2018; Li et al., 2024). GoAstV induces gout and death in goslings within three weeks, and its associated symptoms include depression, anorexia, and the discharge of white, watery stools. Pathological changes are characterized by enlargement of the liver and kidneys and deposition of urate on the surfaces of the internal organs. The virus can cause rapid death in goslings, with a mortality rate reaching as high as 50 %. This virus represents a significant risk to the poultry industry, as there are no available vaccines or effective therapeutic drugs (An et al., 2020; Li et al., 2024; Zhu and Sun, 2022). As such, further research on GoAstV is important to improve poultry performance. The liver is a crucial metabolic organ in poultry, that plays a vital role in viral infections (Zou et al., 2023). Recent research has indicated that GoAstV infection can lead to hepatic damage in goslings. (Xu et al., 2023b). However, detailed studies on the mechanisms underlying liver injury are lacking.

Apoptosis is a complex process (Pistritto et al., 2016) which can be triggered by the stimulation of external or internal pathways. The extrinsic apoptosis pathway is predominantly mediated by the

* Corresponding author.
E-mail address: xqguo20720@jxau.edu.cn (X. Guo).
[1] Theses authors contribute equally to this work.

https://doi.org/10.1016/j.psj.2024.104600
Received 25 September 2024; Accepted 26 November 2024
Available online 27 November 2024

stimulation of cell death receptors such as TNFR. In comparison, the intrinsic apoptosis pathway is mainly driven by the disruption of the mitochondrial membrane, leading to the release of cytochrome C (Wong, 2011). When a viral infection occurs, the host undergoes a dual response, eliminating the virus and hindering viral replication by triggering apoptosis to reduce the spread of the virus to healthy cells. However, the virus interferes with the normal function of host cells through a variety of mechanisms and, in turn, manipulates host cell apoptosis (Shen and Shenk, 1995; Roulston et al., 1999). For example, the N protein of goat parainfluenza virus type 3 (**CPIV3**) has been shown to enhance CPIV3 replication by activating the endogenous and exogenous apoptosis pathways (Li et al., 2021). The V protein of Further, Newcastle disease virus (**NDV**) inhibits apoptosis in a species-specific manner to evade clearance by host cell defense mechanisms (Wang et al., 2018). Viruses can interact with apoptosis through various mechanisms that are crucial for the progression of viral infections and host immune response.

The endoplasmic reticulum (ER) is not only a major site of lipid synthesis, but also of protein folding and maturation. Further, the ER plays a crucial role in intracellular Ca^{2+} storage and signaling, releasing calcium ions through Ryanodine receptors (**RyRs**), inositol 1,4,5-trisphosphate receptors (**IP3Rs**), and recycling calcium ions via proton-pumped sarcoplasmic reticulum Ca^{2+}-ATPase 2 (**SERCA 2**) (Groenendyk et al., 2021). The unfolded protein response (**UPR**) and endoplasmic reticulum stress (ERS) are caused by the disruption of ER homeostasis, dysregulation of calcium metabolism, and increased aggregation of aberrant proteins in the canaliculus lumen following the stimulation of cells by endogenous and exogenous factors such as viruses and hypoxia (Marciniak et al., 2022; Wu et al., 2023). To date, significant evidence points to the critical function of the ER in viral development and replication. Viral agents may use the host cell ER in several ways to accelerate the disruption of correct protein folding, resulting in ERS (Inoue and Tsai, 2013). For example, Coronaviridae viruses utilize the ER as a site for glycoprotein synthesis and genome replication to complete their life cycle (Leyssen et al., 2000; Oostra et al., 2007). Japanese encephalitis viruses influence the folding of ER proteins by altering the structure and number (Hase et al., 1992). Furthermore, the host endoplasmic reticulum is hijacked by the porcine epidemic diarrhea virus (**PEDV**) and coronavirus (**SARS-CoV**) to promote protein replication (DeDiego et al., 2011; Xu et al., 2013). Thus, ERS is of utmost importance in viral infections. However, there is currently no published evidence of an association between GoAstV infection and ERS.

Currently, research on goose astroviruses primarily focuses on the isolation and identification of the virus, as well as the development of vaccines, while reports on the pathogenic mechanism of GoAstV infection causing liver injury are scarce. In the present study, we developed an animal model of GoAstV infection. Based on the liver function indices and histological observations of liver pathology in geese, we explored the mechanisms of ERS and apoptosis in GoAstV-induced liver injury. The objective of this investigation was to offer a theoretical framework for the prevention of GoAstV infection and advancement of vaccines.

Materials and methods

Virus

The GoAstV genotype 2 (GoAstV) strain, isolated by the Institute of Animal Husbandry and Veterinary Medicine, Jiangxi Academy of Agricultural Sciences, with the accession number MZ576222.1 on GenBank (Li et al., 2023a, 2023b, 2023c), was used to establish an infected animal model in this experiment. Virus samples were maintained in a laboratory ultra-low temperature refrigerator.

Animal feeding and sample collection

All procedures were conducted in accordance with the Animal Ethics Committee of Jiangxi Agricultural University (Approval ID: JXAULL-2017003). The Xingguo grey geese used in this investigation were raised in accordance with established norms. One-day-old goslings (n = 200, gray geese, unvaccinated, GoAstV-negative, sex equally divided) were randomly divided into either a control group (**Con**) or a GoAstV-infected group (**Dis**), with 100 geese in each group maintained in two different animal houses with the same conditions. The following day, GoAstV-2 JX01 (2×10^6 $TCID_{50}$/0.2 mL) was subcutaneously injected into all geese in the Dis group, while the same quantity of saline was administered to the Con group. To prevent cross-infection, feeders were divided into two groups throughout the trial, and their clinical symptoms were tracked and examined daily. Eight geese were randomly chosen from each group at 1, 3, 6, and 9 days after injection (fasted and dehydrated for 12 h). After recording body weights and performing blood collection, the animals were euthanized through inhalation of CO_2, and their livers were aseptically removed and weighed for subsequent experiments.

Table 1
qPCR Primer.

Gene	Accession number	Primer sequences (5′ to 3′)
GAPDH	XM_013199522.2	F:GTGCTGCCCAGAACATTATCC R:AGCAGCAGCCTTCACTACCCT
PERK	XM_027455765.2	F:ATTCCCAACTAACCCGAAGGC R:AACCGAAAGTGCTCCATTGCT
ATF6	XM_048080264.1	F:GGCACCTCCCAAAGGTCAAT R:CCGTGACTGAAAGGCTGACT
IRE1	XM_048064614.1	F:GGGAACACCAGCTCAGTAAC R:TCTGGAAGAAATGCTGGCTCTT
GRP78	XM_013188792.2	F:CAGGCTGGTGTTCTCTCTGG R:GGGGACGCTCACCTTCATAG
TRAF2	XM_048053688.1	F:GGAATGCCGGAATCGCT R:ACGTTCCTTTTCCTGGCACA
eIF2α	XM_048059477.1	F:TCGCTTCAGCGTAGCGAGT R:TGTGCCATCTTTAGCAGTTTTCT
ATF4	XM_013181070.1	F:TAGGCAACACCATAGATAGCAGC R:AGATTCAGGGAGATTGGTGATTAG
JNK	XM_027459984.2	F: AGGCTTCTTCCCTGCATCTCC R:ACCACCTACCTGAGCGACCAC
CHOP	XM_048056158.1	F: GCAGTGGCGTAACAGCAAACA R:GCGGAGATTCACTATGCGATTAA
IP3R	XM_048050116.1	F: CCTGTGATGTTGAAGATTGGGAC R:GTTAGGCACATCAGCAACAAAGA
RYR	XM_048047903.1	F: AAGCAGCGATCAGAAGGAGAAA R: ACTTCCTGAACTGATTGGTGCTA
SERCA2α	XM_048073926.1	F: AAGACCGAAAGAGTGTTCAAAGG R: CTTGTCTCCAACTGCCACTTCT
CaMKII	XM_048073825.1	F: CGTGTTTGGGCAGTGTCCTT R: GAAATCTGTAACTTCTGGCTGGTCT
Bax	XM_013195902.2	F: AGGGCTCTTTGCTTGCTTGTG R: TTCGGGGGATAATTTGTGCAT
Bcl-2	XM_048076100.1	F: CTGAGTTTGGTTCTGGTGGGA R: TCCACGATAAACTGGGTGACTCTAC
Caspase-3	XM_048078360.1	F: TCATTCAGGCTTGTAGAGGGACT R: GGAGTAATAGCCTGGAGCAGTAGA
Caspase-9	XM_048067305.1	F: CAGACAAGCCATAATCAGTTTCC R: TGGATGAAGAAGAGTTTGGGTT

Histological staining of the liver

Liver tissues were fixed in 4 % paraformaldehyde, dehydrated in ethanol, and embedded in paraffin. Paraffin-embedded samples then treated to remove the waxy substance and examined using hematoxylin and eosin (**H&E**) staining to observe pathological alterations in the liver using a light microscope.

Ultrastructural analysis

Liver tissues were fixed, dehydrated, embedded, sectioned, and stained in strict accordance with protocols outlined in previous studies (Tian et al., 2023). Finally, ultrastructural observation was performed

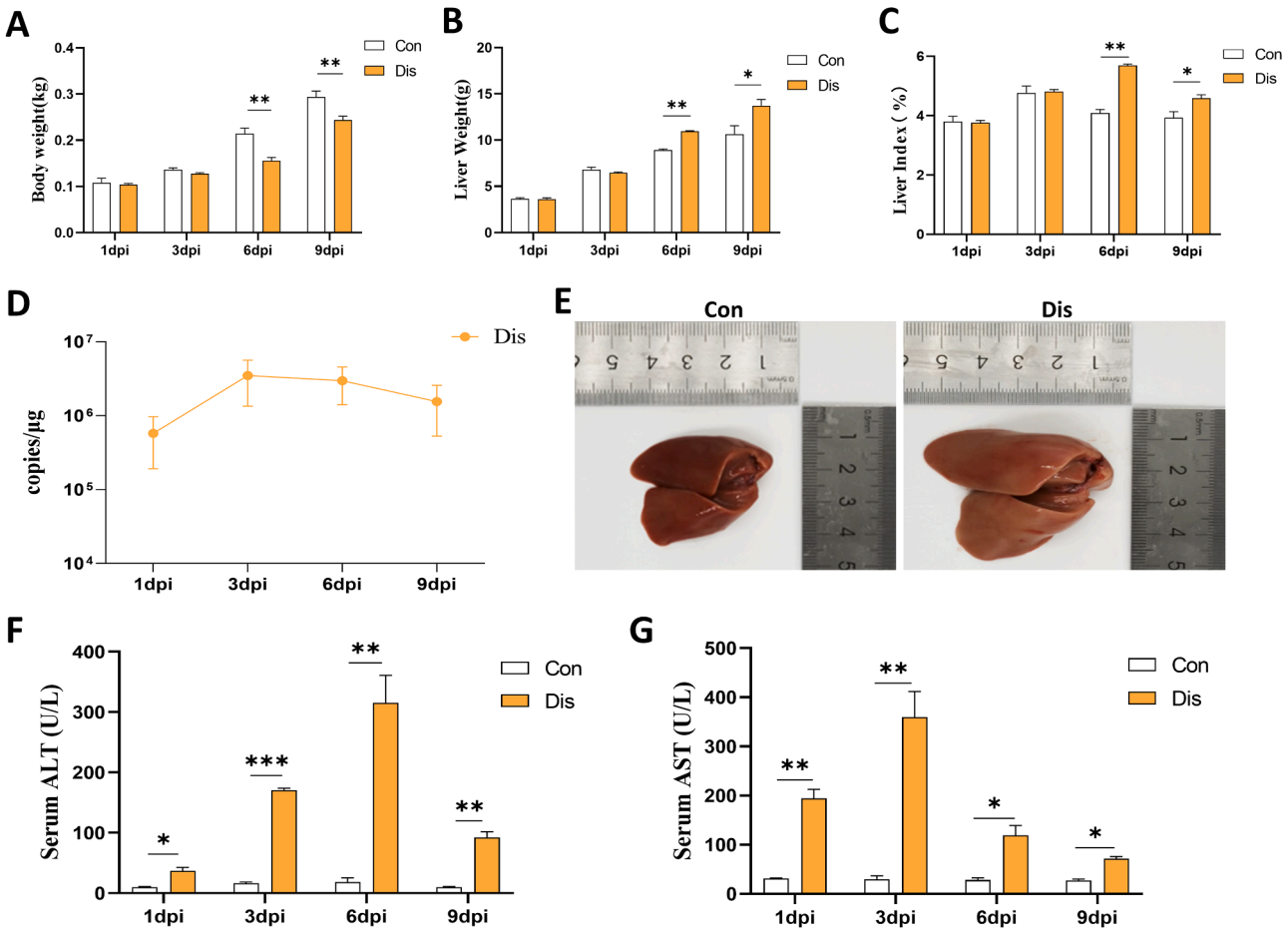

Fig. 1. A-C. Changes of body weight, liver weight and liver coefficients in control and infected groups at 1, 3, 6, 9 dpi. D. Liver viral load. E. Necropsy at 6 dpi showing significant gross pathological changes in the liver. F-G. Changes of AST and ALT activities in serum. All data are expressed as M ± SE and then examined utilizing an independent samples t-test. $P < 0.05$ (*). $P < 0.01$ (**).

by TEM (Hitachi Limited, Japan, HT7700).

RT-qPCR

The manufacturer's instructions (Yeasen Biotechnology, Shanghai, China) were followed to extract total RNA from the liver tissue, which was subsequently reverse-transcribed into cDNA. Table 1 lists the primers used for the target genes. Quantitative PCR was subsequently conducted using cyclic parameters, using a reaction system configured in strict adherence to the amplification system recommended by the RT-qPCR kit (TransGen Biotech, Beijing, China). The mRNA expression levels were determined using $2^{-\Delta\Delta CT}$ and standardized using glyceraldehyde-3-phosphate dehydrogenase (**GAPDH**). In addition, the viral load in the livers of the goslings was determined based on a previous study (Li et al., 2023).

Western blot

Western blotting was performed in accordance with the methodologies described in our previous study (Li et al., 2022). After blocking, membranes were stained with GAPDH, GRP78, IRE1, PERK, ATF6, eIF2α, ATF4, CHOP, JNK, CaMKII, SERCA2, Caspase-3, Caspase-9, Bax, and Bcl-2 primary antibodies (1:1000, Wanlei Biotechnology, Shenyang, China). The membranes were subsequently washed and incubated with appropriate secondary antibodies. Finally, the ECL detection system captured the images. The intensity of each protein band was quantified using the ImageJ software.

Immunohistochemistry

Dewaxing, rehydration, and antigenic thermal repair were performed following the preparation of paraffin-embedded liver slices. Subsequently, 5 % bovine serum protein (Servicebio, Wuhan, China) was added to 3 % H_2O_2, and incubated for 1 h for blocking. The cells were incubated overnight at 4 °C with the primary antibody against IP3R (1:1000, Servicebio, Wuhan, China). After three washes in PBS, the slices were incubated with the designated biotinylated secondary antibody (Servicebio, Wuhan, China) for one hour, and subsequently treated with DAB chromogenic solution. Subsequently, the slices were re-stained with hematoxylin solution, dried, mounted, viewed microscopically, and analyzed using the ImageJ software.

TUNEL staining

After deparaffinization of liver paraffin sections in water, 20 μg/mL proteinase K solution was added dropwise to cover the tissues, and reacted at 37 °C for 15 min, followed by washing with PBS for 5 min and repeated three times. The samples were subsequently treated with 1 % Triton X-100, permeabilized for 3-5 min at room temperature, and washed three times with PBS for 5 min each. The samples were then blotted dry and the experimental samples were washed clean after treatment with the reaction solution from the TUNEL kit (Servicebio, Wuhan, China). Nonspecific coloration of the sections was avoided. Nuclei were re-stained with DAPI (Servicebio, Wuhan, China), washed with PBS, and observed under a fluorescence microscope.

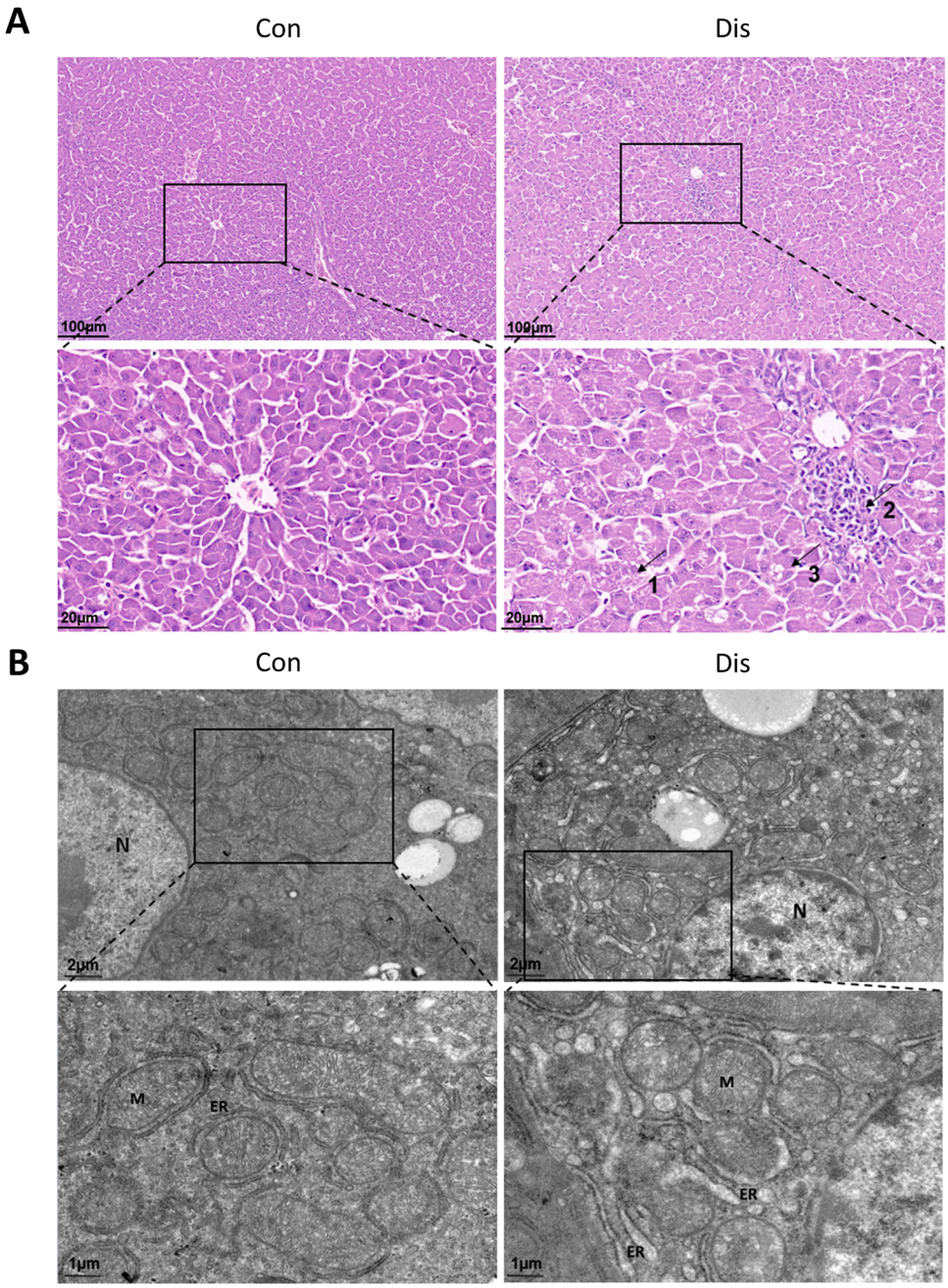

Fig. 2. Effects of GoAstV infection on liver histology and ultrastructure. A. Representative H&E stained sections of liver tissues of both groups at 6 dpi. 1: hepatocyte swelling and rupture, 2: inflammatory cell infiltration, 3: steatosis; Scale bar: 20 μm. B. Observation of the ultrastructure of liver tissues of both groups at 6 dpi. N: nucleus, M: mitochondria, ER: endoplasmic reticulum; Scale bar: 1 μm.

Liver function indicators and tissue calcium content testing

The collected blood was centrifuged to obtain serum samples, after which aspartate aminotransferase (AST) and alanine aminotransferase (ALT) levels were measured using a fully automated biochemical analyzer (Hitachi 3100), in accordance with laboratory standards. Following homogenization of the liver tissue, the hepatic calcium concentration was assessed according to the manufacturer's instructions provided by the kit (Jiancheng Bioengineering Institute, Nanjing, China).

Statistical analysis

There were at least six independent samples in each group, and SPSS 25.0, an analytical software, was employed to conduct independent sample t-test analysis for all test data. GraphPad Prism software (version 9.0) was used to generate graphical findings. $P > 0.05$ indicates no statistically significant differences between the categories. A statistically significant difference between the categories was indicated by $P < 0.05$ (*). $P < 0.01$ (**) indicates highly significant differences between categories. All data are presented as the margin of error (M ± SE) .

Results

Effects of GoAstV infection on physical signs and liver function indexes in goslings

As shown in Fig. 1, the body weight of the Dis group decreased

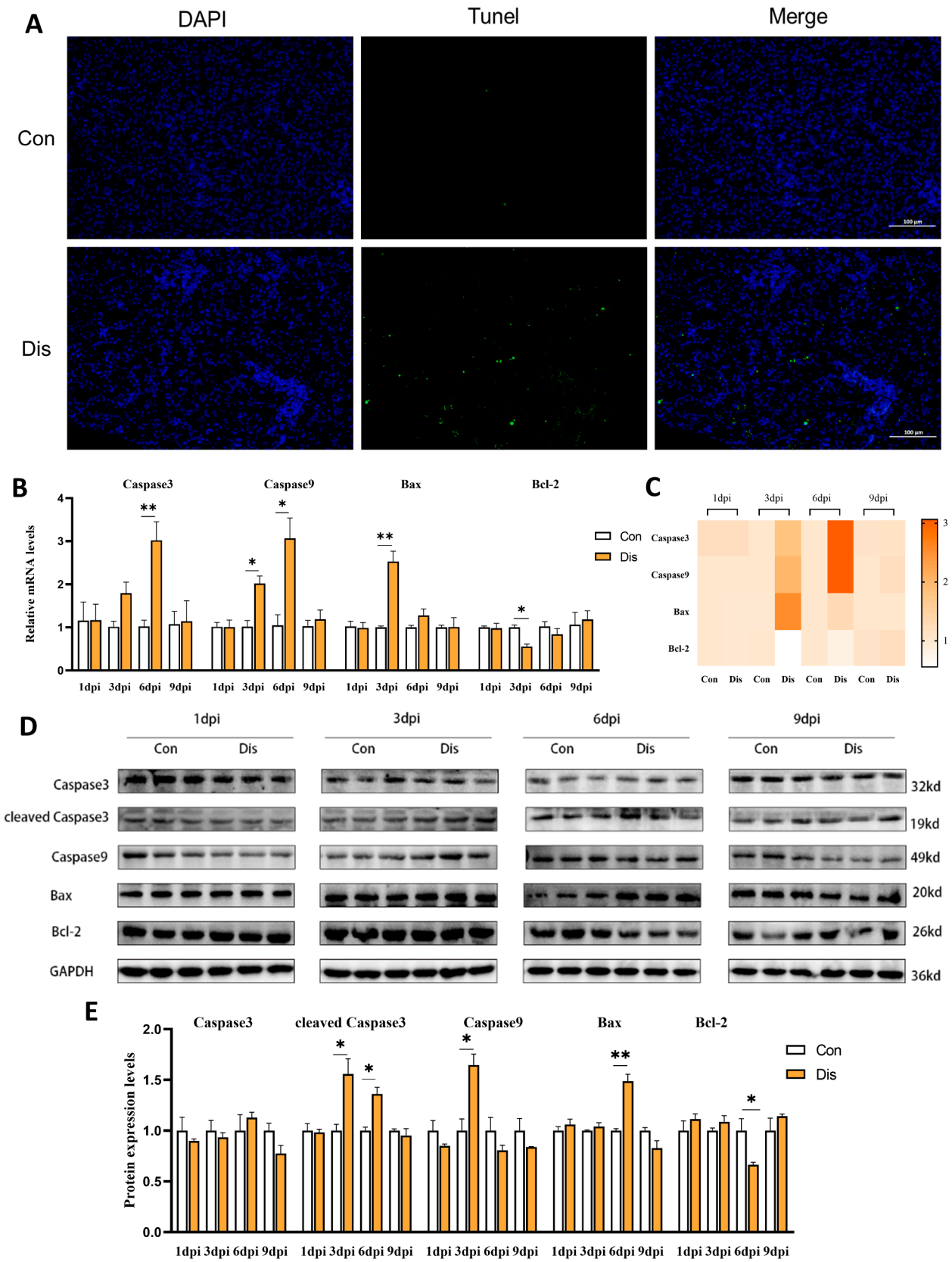

Fig. 3. GoAstV infection induces hepatocyte apoptosis. A. Levels of hepatocyte apoptosis were detected by TUNEL method at 6 dpi. B. Expression levels of mRNA of apoptosis-related genes (Caspase-3, Caspase-9, Bax, and Bcl-2). C. Heatmap indicates the level of change of apoptosis-related genes. D-E. Western blot detection of the relative expression of Caspase-3, cleaved-Caspase-3, Caspase-9, Bax and Bcl-2 proteins. All data are expressed as M ± SE and analyzed using independent samples t-test. $P < 0.05$ (*). $P < 0.01$ (**).

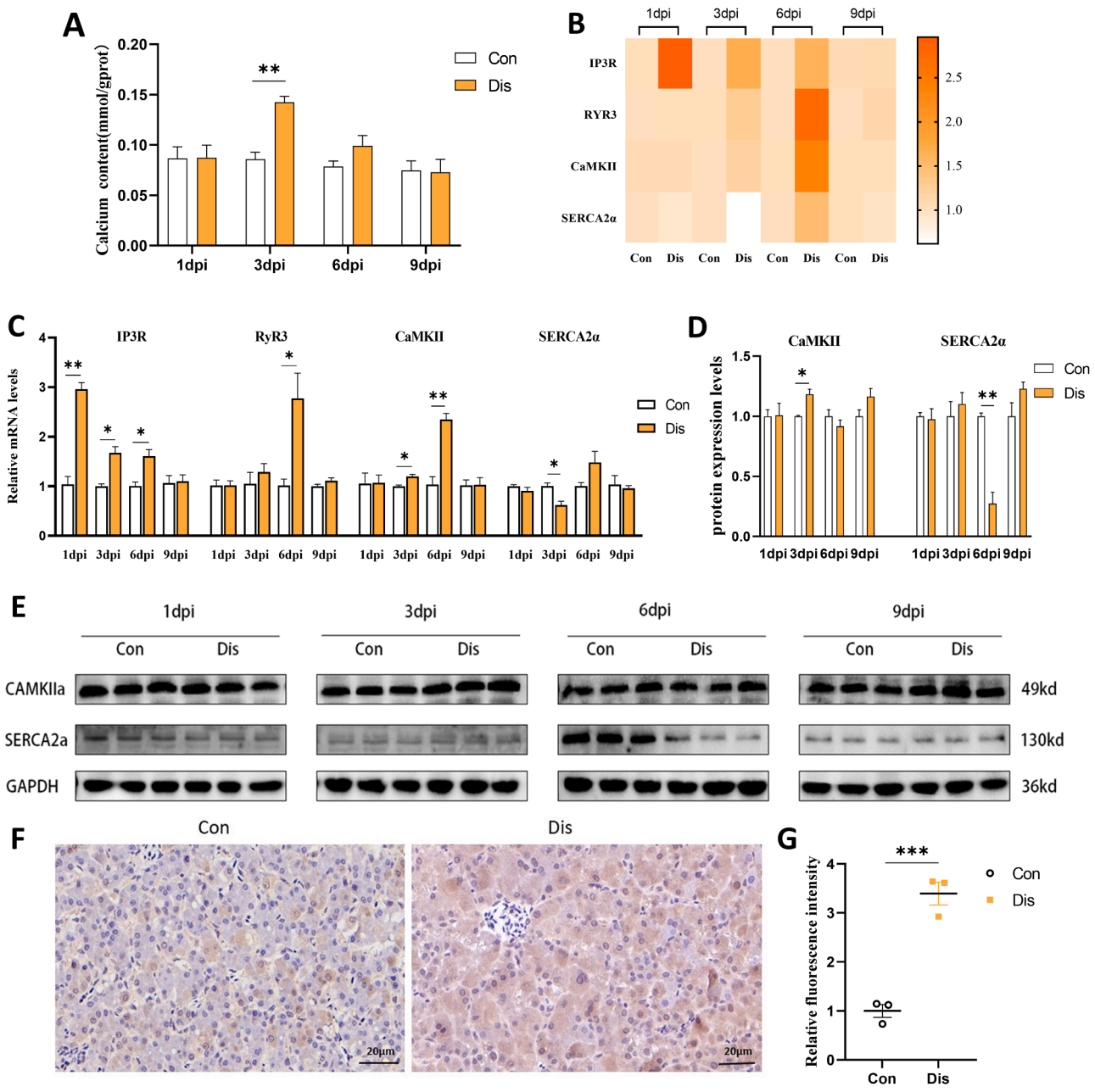

Fig. 4. GoAstV infection can cause liver ER calcium disorders. A. Changes of calcium content in liver tissues of two groups. B. The heatmap illustrates the expression levels of genes associated with ER calcium channels. C. Expression levels of mRNA for ER calcium channel-associated genes (IP3R, RYR3, CaMKII, and SERCA2α). D-F. Western blot analysis to quantify the relative expression levels of CaMKII and SERCA2 proteins. E-F. Immunohistochemical staining at 6 dpi and ImageJ analysis of positive expression of IP3R(Scale bar: 20 μm.B). All data are presented as M ± SE and evaluated using an independent samples t-test. $P < 0.05$ (*). $P < 0.01$ (**).

substantially at 6 and 9 dpi compared with that of the Con group. Additionally, the liver weight and liver index of the Dis group increased significantly at 6 and 9 dpi ($P < 0.01$ and $P < 0.05$, respectively) (Fig. 1A-C). Additionally, dissection revealed that the liver was noticeably enlarged in the Dis group (Fig. 1E). The viral load in the liver reached its highest point at 3 dpi, and progressively declined thereafter (Fig. 1D). The liver function indices ALT and AST exhibited a substantial increase at 1 dpi, with blood enzyme levels remaining elevated at 9 dpi. ($P < 0.01$ or $P < 0.05$) (Fig. 1F-G).

Effects of GoAstV infection on liver histopathology in goslings

Histopathological analysis (Fig. 2A) revealed no significant changes were seen in the Con group, while disorganization of the hepatic cord arrangement, narrowing of the blood sinusoidal space, swelling and rupture of hepatocytes, fatty deterioration, and inflammatory cell infiltration were all observed in the Dis group. In addition, ultrastructural analysis revealed that the organelles were tightly connected, while the endoplasmic reticulum was dilated after GoAstV infection. An unclear nuclear membrane structure was also observed; the nucleus solidified, and the chromatin gradually gathered towards the periphery of the nuclear membrane (Fig. 2B).

Effect of GoAstV infection on apoptosis of foie gras cells

To verify whether GoAstV infection could cause hepatocyte apoptosis, TUNEL staining was conducted, showing that the apoptosis rate in the Dis group was markedly elevated compared to that in the Con

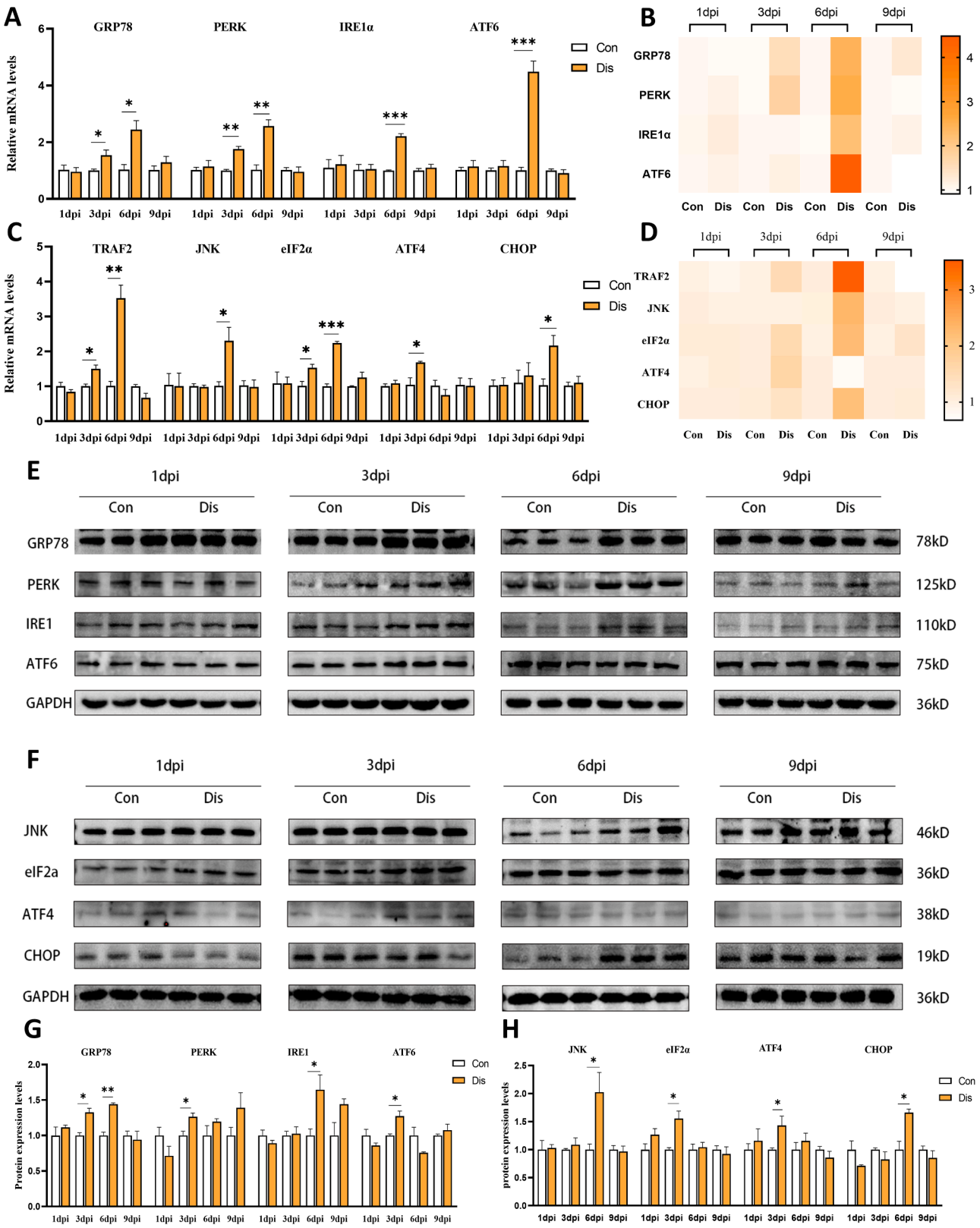

Fig. 5. Effect of GoAstV infection on liver ERS.A and C. Expression levels of genes associated with ERS (GRP78, PERK, IRE1, ATF6, TRAF2, JNK, eIF2α, ATF4 and CHOP). B and D. Heatmaps indicating the mRNA expression levels of ERS-related genes. E-H. Western blot detection of relative expression of GRP78, PERK, IRE1, ATF6, JNK, eIF2α, ATF4 and CHOP proteins. All data are expressed as M±SE and analyzed using independent samples t-test. $P < 0.05$ (*). $P < 0.01$ (**).

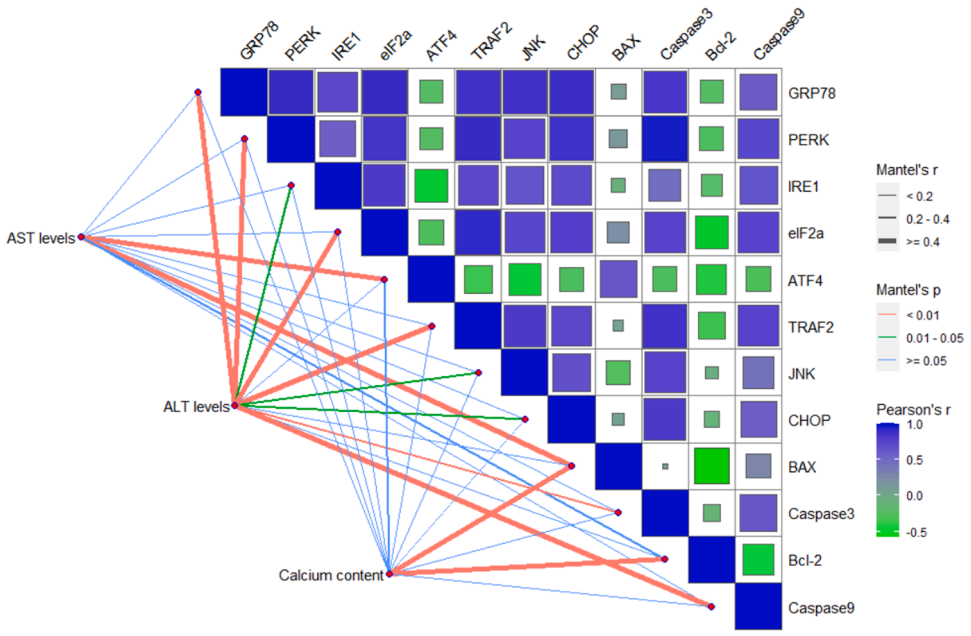

Fig. 6. Correlation examination of mRNA expression levels of the ER stress-related genes and apoptosis-related genes with liver function indices (ALT, AST) and hepatic calcium concentration. Mantel's p denotes the correlation among liver function markers, calcium levels, and several genes. Pearson's r denotes the correlation coefficient between genes linked to ER signaling pathways and genes related to apoptosis.

group (Fig. 3A). Subsequently, the genes and proteins associated with apoptosis were identified. As presented in Fig. 3B-E, we the mRNA expression levels of the pro-apoptosis-related genes Caspase-3, Caspase-9, and Bax showed an overall increasing trend following GoAstV infection. In contrast, mRNA expression of Bcl-2, a gene associated with anti-apoptosis, exhibited a substantial declining trend before returning to normal levels at 9 dpi. Furthermore, relative to the Con group, the protein expression of Cleaved-Caspase-3 in the Dis group was markedly elevated at 3 dpi ($P < 0.05$), while the protein expression levels of Caspase-9, Bcl-2, and Bax corresponded to their gene expression levels.

Effects of GoAstV infection on liver ER calcium in goslings

To examine the impact of GoAstV infection on ER homeostasis in the gosling liver, we assessed hepatic calcium levels and the expression of receptors associated with ER calcium channels. As presented in Fig. 4, the calcium concentration in the Dis group was considerably higher at 3 dpi than in the control group ($P < 0.01$). No significant differences were observed throughout the remainder of the study period (Fig. 4A). A significant increase in the expression of ER calcium release-related genes (IP3R and RYR3) was observed in the Dis group compared with the Con group ($P < 0.01$ or $P < 0.05$). Following infection with GoAstV, there was an increase in the mRNA and protein expression levels of calmodulin kinase (**CaMKII**), as well as the ER calcium uptake protein SERCA2 (Fig. 4B-E). In addition, immunohistochemical analysis revealed a marked elevation in the expression of IP3R protein in the Dis group compared to the Con group ($P < 0.01$) (Fig. 4F-G).

Effects of GoAstV infection on ERS in the livers of goslings

To further investigate whether GoAstV infection induced ERS in the livers of goslings, we analyzed the alterations in the mRNA and protein levels of ERS-related genes. The results are illustrated in Fig. 5. At 3 or 6 dpi, the mRNA expression levels of GRP78, PERK, IRE1, and ATF6 in the Dis group were significantly elevated compared to those in the control group and subsequently returned to normal ($P < 0.01$, or $P < 0.05$) (Fig. 5A-B). The gene expression levels of GRP78, PERK, IRE1, and ATF6 largely agreed with their protein expression levels (Fig. 5E and G). Furthermore, the mRNA expression levels of the downstream genes TRAF2, JNK, eIF2α, ATF4, and CHOP were also detected. The results revealed that the mRNA expression levels in the Dis group initially increased, then decreased, and subsequently returned to normal over time, in contrast to the control group (Fig. 5C-D). Furthermore, the expression levels of JNK, eIF2α, ATF4, and CHOP proteins were comparable to those of mRNA (Fig. 5F and H).

Correlation analysis

Subsequently, to further explore the relationship between GoAstV and ERS-related genes, apoptosis-related genes, liver injury, and ER injury, we plotted the correlation analysis with R4.3.2, the results of which are shown in Fig. 6. Overall, AST levels were highly correlated with the expression of ATF4 and Bax ($P < 0.01$). Further, ALT levels showed a significant association with the expression of GRP78, PERK, eIF2α, TRAF2, and Caspase-9 ($P < 0.01$), whereas the calcium content showed a robust link with the expression of Bax and Bcl-2 ($P < 0.01$). GRP78 showed a strong positive association with JNK, CHOP, and Caspase-3 mRNA expression, whereas PERK showed a significant positive correlation with CHOP and Caspase-3 mRNA expression. Additionally, Bax expression showed a pronounced negative correlation with Bcl-2 mRNA expression.

Discussion

Recently, GoAstV has been reported in the inland provinces of China. Owing to the lack of effective control strategies, it has caused considerable economic damage to the geese industry in these regions. GoAstV infection has been reported to causes urate deposition in goslings, while the liver, the principal organ for uric acid synthesis, is believed to be intricately linked to the virus's pathogenesis (Dalbeth et al., 2021; Zhu and Sun, 2022). The present study aimed to investigate the toxic effects of GoAstV infection on the livers of goslings, focusing on investigating the mechanisms underlying GoAstV infection in the livers of goslings. In the present study, we conducted sectional observation and ultrastructural analyses, and detected hepatic calcium ion concentration levels and levels of related gene proteins in GoAstV-infected goose liver tissues.

The results demonstrated that GoAstV infection in geese leads to liver ERS and hepatocyte apoptosis. These findings are important for exploring the pathogenic mechanisms of GoAstV.

Apoptosis has previously been documented to be intricately linked to several physiological and pathological conditions in the body. It commonly occurs with characteristic morphological changes such as cell volume shrinkage, perinuclear condensation of chromatin, nuclear consolidation, DNA breakage, and fragmentation (Tinari et al., 2008; Cavalcante et al., 2019). In the present study, we performed ultrastructural analysis and TUNEL labeling of liver tissues, observing that the Dis group exhibited the typical features of apoptosis. Moreover, the incidence of apoptosis is largely dependent on the interplay between the Bcl-2 gene family, tumor suppressor genes, and the caspase protease family. The Bcl-2 protein family is crucial for controlling apoptosis. Bax activation is a significant factor that causes mitochondrial MOMP and, in turn, apoptosis. The demise in apoptotic cells is interrupted by the rise of Bcl-2, which together determine cell survival and death (Tait and Green, 2010; Li and Dewson, 2015). Caspase-9 and Caspase-3 are apoptosis-initiating and-executing enzymes, respectively, both of which are closely associated with the mitochondrial apoptotic pathway (Del Puerto et al., 2011; Li et al., 2017). Prior research has demonstrated that NIBV induces apoptosis in chick-derived kidney cells by activating Bax, Caspase-9, and Caspase-3, while inhibiting Bcl-2 expression activity (Chen et al., 2022b). ISKNV infection induces the interaction of Bax and Bcl-2 to activate signal transduction between Caspase-9 and Caspase-3, resulting in the apoptosis of GF-1 cells (Chen et al., 2022a). Increasing evidence suggests that viral infections, such as HIV and influenza virus infections, can either directly or indirectly induce the activation of Caspase-9 and Caspase-3, triggering apoptosis through multiple mechanisms (Mehrbod et al., 2019). The present study demonstrated that following GoAstV infection, the mRNA and protein levels of Bax, Caspase-3, and Caspase-9 were elevated, whereas Bcl-2 expression was markedly reduced. It has further been suggested that infection with GoAstV activates the mitochondrial apoptotic pathway, resulting in apoptosis of liver cells. However, the exact mechanism underlying apoptosis induction requires further investigation.

Prior research has shown that most positive-stranded RNA viruses rely predominantly on the ER for replication and maturation of their proteins during infection. Viruses create environments that support the maturation of replicative complexes or viral particles, by inducing changes in the ER structure and stimulating fatty acid synthesis (Verchot, 2016). In the present study, disorganization of the ER structure in the Dis group was observed through electron microscopy, indicating that ER function is impaired, or that ER homeostasis may be disrupted. The balance of Ca^{2+} concentration is an important condition for maintaining homeostasis in the ER (Mekahli et al., 2011). Furthermore, there have been reports showing that viral infections are commonly accompanied by disturbances in Ca^{2+} concentration, resulting impaired cellular function (Olivier, 1996). The Dis group exhibited a substantial increase in hepatic Ca^{2+} content at 6 dpi compared to the Con group, as indicated by our findings. This suggests that GoAstV infection caused a disturbance in the Ca^{2+} concentration in the liver tissue of goslings. Under normal conditions, the cytoplasmic Ca^{2+} concentration is maintained at a low level, whereas the ER and extracellular interstitial Ca^{2+} concentrations are higher (Bagur and Hajnóczky, 2017). The SERCA pump is largely responsible for the absorption of cytoplasmic Ca^{2+} into the ER, whereas the IP3R and RyR channels located in the ER membrane are primarily responsible for facilitating the release of calcium ions from the ER lumen into the cytoplasm. Evidence has demonstrated that some viruses can enhance the release of Ca^{2+} by upregulating RyR or IP3R expression. Research indicates that some viruses may enhance Ca^{2+} release by elevating the expression of RyR or IP3R while concurrently diminishing SERCA function, thereby aggravating calcium ion imbalance in the endoplasmic reticulum and eventually facilitating viral replication (Mekahli et al., 2011). For example, the presence of hepatitis C virus (**HCV**) and Borna disease virus (**BDV**) may result in a reduction in SERCA activity. (Benali-Furet et al., 2005; Williams and Lipkin, 2006), whereas poliovirus (**PV**) and influenza A virus (**IAV**) can cause an increase in IP3R or RYR activity (Hartshorn et al., 1988; Guinea et al., 1989). In addition, infection with porcine circovirus type 2 (**PCV2**) stimulates CaMKII expression by increasing cytoplasmic Ca^{2+} levels (Gu et al., 2016). They regulate the ER Ca^{2+} concentration, thereby creating favorable conditions for viral survival. This illustrates the importance of ER Ca^{2+} regulation in viral infections.

The present work revealed that GoAstV infection triggered an increase in the mRNA expression of IP3R, RYR3, and CaMKII, while decreasing the mRNA activity of SERCA2α, through the analysis of calcium-related channel receptors on the ER membrane. In addition, a notable elevation in CaMKII protein levels and a substantial reduction in SERCA translation were observed. The positive expression of IP3R observed in the immunohistochemical results generally agreed with the aforementioned findings. In conclusion, these results demonstrate that during GoAstV infection, damage to the ER structure of the goose liver causes ER Ca^{2+} depletion, resulting in an imbalance in the ER Ca^{2+} concentration.

Ca^{2+} is one of the key factors ensuring the proper folding of ER proteins, and the depletion of ER Ca^{2+} affects the folding ability of ER proteins to some extent (Gaut and Hendershot, 1993). In addition, previous studies have shown that ER Ca^{2+} depletion robustly activates ERS and the UPR (Hammadi et al., 2013). In a healthy physiological state, GRP78 binds to PERK, ATF6, and IRE1 in an inactive state. When ERS is triggered, PERK, ATF6, and IRE1 are activated and dissociate from GRP78 to initiate the UPR. It has been reported that ERS triggered by most viruses, including hepatitis B virus (**HBV**) and dengue virus (**DENV**), can simultaneously activate the three transmembrane sensors of the UPR. However, some viruses, such as SARS-CoV and flavivirus (DENV), can only activate one or two branches of the UPR (Li et al., 2015). In the present study, GoAstV was found to upregulate the mRNA and protein levels of GRP78, PERK, IRE1, and ATF6 in geese, which returned to normal levels post-infection. This result suggests that GoAstV infection can cause hepatic ERS and UPR, activating the PERK, IRE1, and ATF6 signaling axes.

The association between ERS stress and apoptosis is complex. Mild ERS may activate adaptive responses for cell survival to protect the cells from stress-induced damage. Conversely, severe ERS can interact with and regulate apoptotic processes each other (Almanza et al., 2019). Currently, several signaling mechanisms in the ER have been shown to induce apoptosis, including the Caspase, CHOP, and JNK pathways (Li et al., 2006). The activation of the eIF2α-ATF4-CHOP signaling pathway is pivotal in initiating apoptotic processes in cells infected by human astrovirus (Isobe et al., 2019). The expression of Bax or Bcl-2 genes can further be altered to induce apoptosis through the up-regulation of CHOP, either directly or indirectly (Ron, 2002; Oyadomari and Mori, 2004). Furthermore, increasing evidence suggests that viruses can modulate the TRAF2-JNK signaling pathway through various mechanisms to enhance their replication. JNK activation plays a crucial role in the endogenous apoptotic pathway (Chen et al., 2021). The results of the present study demonstrated a trend of up-regulation of mRNA levels of eIF2α, ATF4, CHOP, TRAF2, and JNK, as well as protein levels of ATF4, eIF2α, CHOP, and JNK in the infected group, indicating that infection of goslings with GoAstV activates the IRE1-TRAF2 and PERK-eIF2α-ATF4 signaling axes, and promotes the expression of JNK and CHOP. Furthermore, correlation analysis revealed a strong positive association between GRP78 and mRNA expression levels of JNK and Caspase-3. Similarly, PERK expression exhibited a robust positive correlation with the mRNA expression of CHOP and Caspase-3. Conversely, Bax expression was found to be negatively correlated with Bcl-2 expression. These data suggest that GoAstV infection amplifies the activation of CHOP and JNK, which is possibly associated with the GoAstV-induced apoptosis of hepatocytes. However, whether ERS is involved in GoAstV-mediated goose hepatocyte apoptosis remains unclear.

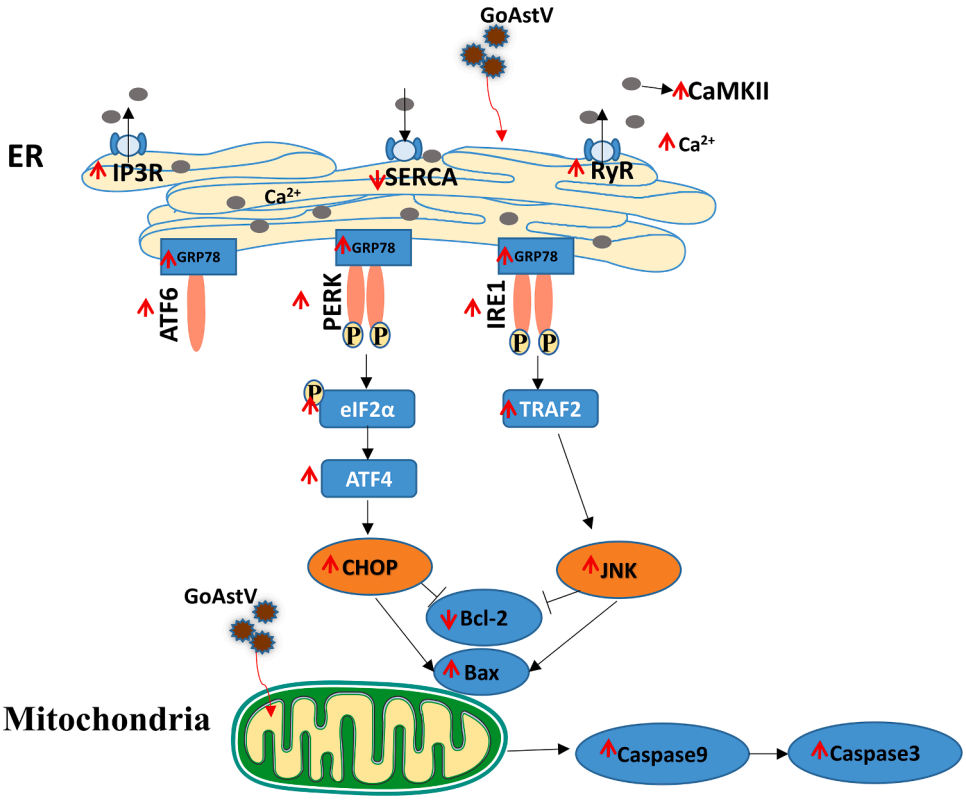

Fig. 7. ERS and apoptosis signaling in GoAstV infection.

Conclusion

In conclusion, our results indicate that GoAstV intensifies the occurrence of ERS by interfering with the ER Ca^{2+} balance, leading to hepatocyte apoptosis in infected goslings. Furthermore, GoAstV infection induces apoptosis in gosling liver cells, which may be related to the activation of the ERS pathway. Taken together, these findings provide insight into the mechanism of liver injury caused by GoAstV infection. Based on the results of the present study, the signal maps of ERS and apoptosis were mapped (Fig. 7).

Disclosures

We know of no conflicts of interest associated with this publication, and I confirm that the manuscript has been read and approved for submission by all named authors.

Declaration of competing interest

The authors declare that the research was conducted in the absence of any commercial or financial relationships that could be construed as a potential conflict of interest.

Acknowledgments

This work was supported by National Natural Science Foundation of China (32360875 and 32072935), Jiangxi Provincial Natural Science Foundation (20242BAB25394), basic research and talent training of Jiangxi Academy of Agricultural Sciences (JXSNKYJCRC202205), Jiangxi Agriculture Research System (JXARS), the Innovation Team of Jiangxi Agricultural University (JXAUCXTD006), and Jiangxi Provincial Key R&D Program Project (20224BBF62003).

Supplementary materials

Supplementary material associated with this article can be found, in the online version, at doi:10.1016/j.psj.2024.104600.

References

Almanza, A., Carlesso, A., Chintha, C., Creedican, S., Doultsinos, D., Leuzzi, B., Luís, A., McCarthy, N., Montibeller, L., More, S., Papaioannou, A., Püschel, F., Sassano, M.L., Skoko, J., Agostinis, P., de Belleroche, J., Eriksson, L.A., Fulda, S., Gorman, A.M., Healy, S., Kozlov, A., Muñoz-Pinedo, C., Rehm, M., Chevet, E., Samali, A., 2019. Endoplasmic reticulum stress signalling - from basic mechanisms to clinical applications. Febs. J. 286, 241–278.

An, D., Zhang, J., Yang, J., Tang, Y., Diao, Y., 2020. Novel goose-origin astrovirus infection in geese: the effect of age at infection. Poult. Sci. 99, 4323–4333.

Bagur, R., Hajnóczky, G., 2017. Intracellular Ca^{2+} Sensing: its Role in Calcium Homeostasis and Signaling. Mol. Cell 66, 780–788.

Benali-Furet, N.L., Chami, M., Houel, L., De Giorgi, F., Vernejoul, F., Lagorce, D., Buscail, L., Bartenschlager, R., Ichas, F., Rizzuto, R., Paterlini-Bréchot, P., 2005. Hepatitis C virus core triggers apoptosis in liver cells by inducing ER stress and ER calcium depletion. Oncogene 24, 4921–4933.

Cavalcante, G.C., Schaan, A.P., Cabral, G.F., Santana-da-Silva, M.N., Pinto, P., Vidal, A. F., Ribeiro-Dos-Santos, Â., 2019. A cell's fate: an overview of the molecular biology and genetics of apoptosis. Int. J. Mol. Sci. 20.

Chen, J., Ye, C., Wan, C., Li, G., Peng, L., Peng, Y., Fang, R., 2021. The roles of c-Jun N-terminal kinase (JNK) in infectious diseases. Int. J. Mol. Sci. 22.

Chen, P.H., Hsueh, T.C., Wu, J.L., Hong, J.R., 2022a. Infectious spleen and kidney necrosis virus (ISKNV) triggers mitochondria-mediated dynamic interaction signals via an imbalance of bax/Bak over Bcl-2/Bcl-xL in fish cells. Viruses 14.

Chen, W., Huang, C., Shi, Y., Li, N., Wang, E., Hu, R., Li, G., Yang, F., Zhuang, Y., Liu, P., Hu, G., Gao, X., Guo, X., 2022b. Investigation of the crosstalk between GRP78/PERK/ATF-4 signaling pathway and renal apoptosis induced by nephropathogenic infectious bronchitis virus infection. J. Virol. 96, e0142921.

Dalbeth, N., Gosling, A.L., Gaffo, A., Abhishek, A., 2021. Gout. Lancet 397, 1843–1855.

DeDiego, M.L., Nieto-Torres, J.L., Jiménez-Guardeño, J.M., Regla-Nava, J.A., Alvarez, E., Oliveros, J.C., Zhao, J., Fett, C., Perlman, S., Enjuanes, L., 2011. Severe acute respiratory syndrome coronavirus envelope protein regulates cell stress response and apoptosis. PLoS Pathog. 7, e1002315.

Del Puerto, H.L., Martins, A.S., Milsted, A., Souza-Fagundes, E.M., Braz, G.F., Hissa, B., Andrade, L.O., Alves, F., Rajão, D.S., Leite, R.C., Vasconcelos, A.C., 2011. Canine distemper virus induces apoptosis in cervical tumor derived cell lines. Virol. J. 8, 334.

Gaut, J.R., Hendershot, L.M., 1993. The modification and assembly of proteins in the endoplasmic reticulum. Curr. Opin. Cell Biol. 5, 589–595.
Groenendyk, J., Agellon, L.B., Michalak, M., 2021. Calcium signaling and endoplasmic reticulum stress. Int. Rev. Cell Mol. Biol. 363, 1–20.
Gu, Y., Qi, B., Zhou, Y., Jiang, X., Zhang, X., Li, X., Fang, W., 2016. Porcine circovirus Type 2 activates CaMMKβ to initiate autophagy in PK-15 cells by increasing cytosolic calcium. Viruses. 8.
Guinea, R., López-Rivas, A., Carrasco, L., 1989. Modification of phospholipase C and phospholipase A2 activities during poliovirus infection. J. Biol. Chem. 264, 21923–21927.
Hammadi, M., Oulidi, A., Gackière, F., Katsogiannou, M., Slomianny, C., Roudbaraki, M., Dewailly, E., Delcourt, P., Lepage, G., Lotteau, S., Ducreux, S., Prevarskaya, N., Van Coppenolle, F., 2013. Modulation of ER stress and apoptosis by endoplasmic reticulum calcium leak via translocon during unfolded protein response: involvement of GRP78. FASEB J. 27, 1600–1609.
Hartshorn, K.L., Collamer, M., Auerbach, M., Myers, J.B., Pavlotsky, N., Tauber, A.I., 1988. Effects of influenza A virus on human neutrophil calcium metabolism. J. Immunol. 141, 1295–1301.
Hase, T., Summers, P.L., Ray, P., Asafo-Adjei, E., 1992. Cytopathology of PC12 cells infected with Japanese encephalitis virus. Virchows Arch. B Cell Pathol. Incl. Mol. Pathol. 63, 25–36.
Inoue, T., Tsai, B., 2013. How viruses use the endoplasmic reticulum for entry, replication, and assembly. Cold. Spring. Harb. Perspect. Biol. 5, a013250.
Isobe, T., Tange, S., Tasaki, H., Kanamori, K., Kato, A., Nakanishi, A., 2019. Upregulation of CHOP participates in Caspase activation and virus release in human astrovirus-infected cells. J. Gen. Virol. 100, 778–792.
Leyssen, P., De Clercq, E., Neyts, J., 2000. Perspectives for the treatment of infections with flaviviridae. Clin. Microbiol. Rev. 13, 67–82 table of contents.
Li, H., Kang, Z., Wan, C., Zhang, F., Tan, M., Zeng, Y., Wu, C., Huang, Y., Su, Q., Guo, X., 2023a. Rapid diagnosis of different goose astrovirus genotypes with Taqman-based duplex real-time quantitative PCR. Poult. Sci. 102, 102730.
Li, H., Su, Q., Fu, D., Huang, H., Lu, Z., Huang, C., Chen, Y., Tan, M., Huang, J., Kang, Z., Wei, Q., Guo, X., 2024. Alteration of gut microbiome in goslings infected with goose astrovirus. Poult. Sci. 103, 103869.
Li, H., Wan, C., Wang, Z., Tan, J., Tan, M., Zeng, Y., Huang, J., Huang, Y., Su, Q., Kang, Z., Guo, X., 2023b. Rapid diagnosis of duck Tembusu virus and goose astrovirus with TaqMan-based duplex real-time PCR. Front. Microbiol. 14, 1146241.
Li, H., Zhu, Y., Wan, C., Wang, Z., Liu, L., Tan, M., Zhang, F., Zeng, Y., Huang, J., Wu, C., Huang, Y., Kang, Z., Guo, X., 2023c. Rapid detection of goose astrovirus genotypes 2 using real-time reverse transcription recombinase polymerase amplification. BMC Vet. Res. 19, 232.
Li, J., Lee, B., Lee, A.S., 2006. Endoplasmic reticulum stress-induced apoptosis: multiple pathways and activation of p53-up-regulated modulator of apoptosis (PUMA) and NOXA by p53. J. Biol. Chem. 281, 7260–7270.
Li, J., Yang, L., Mao, L., Li, W., Sun, M., Liu, C., Xue, T., Zhang, W., Liu, M., Li, B., 2021. Caprine parainfluenza virus type 3 N protein promotes viral replication via inducing apoptosis. Vet. Microbiol. 259, 109129.
Li, M.X., Dewson, G., 2015. Mitochondria and apoptosis: emerging concepts. F1000 Prime Rep. 7, 42.
Li, N., Huang, C., Chen, W., Li, Z., Hu, G., Li, G., Liu, P., Hu, R., Zhuang, Y., Luo, J., Gao, X., Guo, X., 2022. Nephropathogenic infectious bronchitis virus mediates kidney injury in chickens via the TLR7/NF-κB signaling axis. Front. Cell Infect. Microbiol. 12, 865283.
Li, S., Kong, L., Yu, X., 2015. The expanding roles of endoplasmic reticulum stress in virus replication and pathogenesis. Crit. Rev. Microbiol. 41, 150–164.
Li, Y., Zhou, M., Hu, Q., Bai, X.C., Huang, W., Scheres, S.H., Shi, Y., 2017. Mechanistic insights into caspase-9 activation by the structure of the apoptosome holoenzyme. Proc. Natl. Acad. Sci. U.S.A. 114, 1542–1547.
Marciniak, S.J., Chambers, J.E., Ron, D., 2022. Pharmacological targeting of endoplasmic reticulum stress in disease. Nat. Rev. Drug Discov. 21, 115–140.
Mehrbod, P., Ande, S.R., Alizadeh, J., Rahimizadeh, S., Shariati, A., Malek, H., Hashemi, M., Glover, K.K.M., Sher, A.A., Coombs, K.M., Ghavami, S., 2019. The roles of apoptosis, autophagy and unfolded protein response in arbovirus, influenza virus, and HIV infections. Virulence 10, 376–413.
Mekahli, D., Bultynck, G., Parys, J.B., De Smedt, H., Missiaen, L., 2011. Endoplasmic-reticulum calcium depletion and disease. Cold. Spring. Harb. Perspect. Biol. 3.
Niu, X., Tian, J., Yang, J., Jiang, X., Wang, H., Chen, H., Yi, T., Diao, Y., 2018. Novel goose astrovirus associated gout in gosling, China. Vet. Microbiol. 220, 53–56.
Olivier, M., 1996. Modulation of host cell intracellular Ca^{2+}. Parasitol. Today 12, 145–150.
Oostra, M., te Lintelo, E.G., Deijs, M., Verheije, M.H., Rottier, P.J., de Haan, C.A., 2007. Localization and membrane topology of coronavirus nonstructural protein 4: involvement of the early secretory pathway in replication. J. Virol. 81, 12323–12336.
Oyadomari, S., Mori, M., 2004. Roles of CHOP/GADD153 in endoplasmic reticulum stress. Cell Death. Differ. 11, 381–389.
Pistritto, G., Trisciuoglio, D., Ceci, C., Garufi, A., D'Orazi, G., 2016. Apoptosis as anticancer mechanism: function and dysfunction of its modulators and targeted therapeutic strategies. Aging (Albany NY) 8, 603–619.
Ron, D., 2002. Translational control in the endoplasmic reticulum stress response. J. Clin. Invest. 110, 1383–1388.
Roulston, A., Marcellus, R.C., Branton, P.E., 1999. Viruses and apoptosis. Annu. Rev. Microbiol. 53, 577–628.
Shen, Y., Shenk, T.E., 1995. Viruses and apoptosis. Curr. Opin. Genet. Dev. 5, 105–111.
Tait, S.W., Green, D.R., 2010. Mitochondria and cell death: outer membrane permeabilization and beyond. Nat. Rev. Mol. Cell Biol. 11, 621–632.
Tian, G., Huang, C., Li, Z., Lu, Z., Feng, C., Zhuang, Y., Li, G., Liu, P., Hu, G., Gao, X., Guo, X., 2023. Baicalin mitigates nephropathogenic infectious bronchitis virus infection-induced spleen injury via modulation of mitophagy and macrophage polarization in Hy-Line chick. Vet. Microbiol. 286, 109891.
Tinari, A., Giammarioli, A.M., Manganelli, V., Ciarlo, L., Malorni, W., 2008. Analyzing morphological and ultrastructural features in cell death. Methods Enzymol. 442, 1–26.
Verchot, J., 2016. How does the stressed out ER find relief during virus infection? Curr. Opin. Virol. 17, 74–79.
Wang, C., Chu, Z., Liu, W., Pang, Y., Gao, X., Tang, Q., Ma, J., Lu, K., Adam, F.E.A., Dang, R., Xiao, S., Wang, X., Yang, Z., 2018. Newcastle disease virus V protein inhibits apoptosis in DF-1 cells by downregulating TXNL1. Vet. Res. 49, 102.
Williams, B.L., Lipkin, W.I., 2006. Endoplasmic reticulum stress and neurodegeneration in rats neonatally infected with borna disease virus. J. Virol. 80, 8613–8626.
Wong, R.S., 2011. Apoptosis in cancer: from pathogenesis to treatment. J. Exp. Clin. Cancer Res. 30, 87.
Wu, D., Huang, L.F., Chen, X.C., Huang, X.R., Li, H.Y., An, N., Tang, J.X., Liu, H.F., Yang, C., 2023. Research progress on endoplasmic reticulum homeostasis in kidney diseases. Cell Death. Dis. 14, 473.
Xu, L., Jiang, B., Cheng, Y., Gao, Z., He, Y., Wu, Z., Wang, M., Jia, R., Zhu, D., Liu, M., Zhao, X., Yang, Q., Wu, Y., Zhang, S., Huang, J., Ou, X., Gao, Q., Sun, D., Cheng, A., Chen, S., 2023a. Molecular epidemiology and virulence of goose astroviruses genotype-2 with different internal gene sequences. Front. Microbiol. 14, 1301861.
Xu, L., Jiang, B., Cheng, Y., He, Y., Wu, Z., Wang, M., Jia, R., Zhu, D., Liu, M., Zhao, X., Yang, Q., Wu, Y., Zhang, S., Huang, J., Mao, S., Ou, X., Gao, Q., Sun, D., Cheng, A., Chen, S., 2023b. Infection and innate immune mechanism of goose astrovirus. Front. Microbiol. 14, 1121763.
Xu, X., Zhang, H., Zhang, Q., Dong, J., Liang, Y., Huang, Y., Liu, H.J., Tong, D., 2013. Porcine epidemic diarrhea virus E protein causes endoplasmic reticulum stress and up-regulates interleukin-8 expression. Virol. J. 10, 26.
Yang, J., Tian, J., Tang, Y., Diao, Y., 2018. Isolation and genomic characterization of gosling gout caused by a novel goose astrovirus. Transbound. Emerg. Dis. 65, 1689–1696.
Zhang, Y., Wang, F., Liu, N., Yang, L., Zhang, D., 2017. Complete genome sequence of a novel avastrovirus in goose. Arch. Virol. 162, 2135–2139.
Zhu, Q., Sun, D., 2022. Goose astrovirus in China: a comprehensive review. Viruses. 14.
Zou, J., Li, J., Zhong, X., Tang, D., Fan, X., Chen, R., 2023. Liver in infections: a single-cell and spatial transcriptomics perspective. J. Biomed. Sci. 30, 53.